Journal of Alloys and Compounds 526 (2012) 125–128

Contents lists available at SciVerse ScienceDirect

Journal of Alloys and Compounds

journal homepage: www.elsevier.com/locate/jallcom

Crystal structure and physical properties of Ce_3Rh_5Si

A. Lipatov[a], D. Kaczorowski[b,*], A. Gribanov[a], Y. Seropegin[a]

[a] Department of Chemistry, Moscow State University, GSP-1, 119991 Moscow, Russia
[b] Institute of Low Temperature and Structure Research, Polish Academy of Sciences, P.O. Box 1410, 50-950 Wrocław, Poland

ARTICLE INFO

Article history:
Received 21 January 2012
Received in revised form 10 February 2012
Accepted 13 February 2012
Available online xxx

Keywords:
Cerium intermetallics
Magnetic behavior
Electrical resistivity

ABSTRACT

The crystal structure of the novel compound Ce_3Rh_5Si was solved by means of powder diffraction pattern analysis using the charge-flipping method. The refinements yielded the space group *Pnma* and the orthorhombic unit cell parameters: $a = 1.52632(2)$ nm, $b = 0.55092(1)$ nm, and $c = 0.75302(1)$ nm. A characteristic feature of the crystal structure of Ce_3Rh_5Si are vertex-sharing $[Rh_4]$ and $[Rh_3Si]$ tetrahedra, which form a three-dimensional framework with Ce atoms located inside truncated tetrahedral voids. The structure exhibits close relationship with those of $CeRh_2$ ($MgCu_2$-type) and Ce_2Rh_3Si (Y_2Rh_3Si-type). Magnetic and electrical resistivity measurements of Ce_3Rh_5Si were performed down to 2 K. The compound was characterized as a Pauli paramagnet with metallic character of the electrical conductivity.

1. Introduction

Recently, the ternary phase diagram Ce–Rh–Si has been carefully investigated and the formation of several novel compounds has been established [1]. Among them is a phase with the composition within the range 8.5–11.5 at.% of Si and 33 at.% of Ce, which has been identified to bear close structural relationship with the orthorhombic low-temperature modification of UMn_2, yet at that time its exact crystal structure could not be solved because of metallurgical problems in obtaining single-phase material. Here, we report on the crystal structure refinements made for high-quality polycrystalline sample. Moreover, we describe the primary magnetic and electrical properties of the new phase.

2. Experimental

Polycrystalline sample of Ce_3Rh_5Si was prepared by arc-melting high-purity elements (99.8 mass % Ce, 99.999 mass % Si and 99.99 mass % Rh) on a water-cooled copper hearth under argon atmosphere. To promote homogeneity, the melting was repeated several times with the button turned over between each melting. The final weight loss was less than 0.2 mass %. Subsequently, the alloy was vacuum-sealed in a quartz tube and annealed at 950 °C for 2 weeks. The heat treatment was finished with quenching in cold water.

The powder X-ray diffraction (XRD) data were collected at room temperature employing a STOE STADI P transmission diffractometer, equipped with a linear position sensitive detector (monochromatic $CuK\alpha_1$ radiation with $\lambda = 1.54056$ Å; $10^\circ \le 2\theta \le 90^\circ$). The sample was also examined by energy-dispersive X-ray analysis (EDX) using a Carl Zeiss LEO EVO 50XVP scanning electron microscope equipped with a Link EDX INCA Energy 450 system (Q-BSD detector).

Magnetic measurements were carried out over the temperature interval 2–400 K in magnetic fields up to 5 T employing a Quantum Design MPMS-5 SQUID magnetometer. The electrical resistivity was measured from 2 to 300 K by a conventional four-probe dc technique implemented in a home-made setup. Electrical leads (copper wires) were attached to the bar-shaped specimens using silver-epoxy paste.

3. Results and discussion

3.1. Crystal structure

The lattice parameters were refined from the powder XRD data employing the program WinXPOW [2]. The obtained values $a = 1.5284(1)$ nm, $b = 0.5511(1)$ nm, $c = 0.7536(1)$ nm are in good agreement with those reported in Ref. [1]. Further analysis of the X-ray pattern was carried out using the FULLPROF program [3], and the charge-flipping algorithm implemented in the program SUPERFLIP [4]. The structure was solved in the centrosymmetric space group *Pnma* and refined down to $R_F = 0.055$. The refined X-ray diffraction pattern is presented in Fig. 1. The key data on the experimental conditions and the performed calculations are gathered in Table 1. The refined atomic coordinates and isotropic thermal displacement parameters are listed in Table 2, while the main interatomic distances in the refined unit cell are given in Table 3. The crystal structure of Ce_3Rh_5Si as well as the coordination polyhedra for each type of atom are presented in Fig. 2. As can be inferred from this figure, the Ce atoms occupy three distinct positions in the unit cell. All of them are located in truncated tetrahedral voids made by vertex-sharing $[Rh_4]$ and $[Rh_3Si]$ tetrahedra. Remarkably, the Rh atoms being engaged in the formation of the rigid three dimensional framework of the crystal structure exhibit distinctly smaller

---

* Corresponding author. Tel.: +48 71 34 350 21; fax: +48 71 34 410 19.
E-mail address: D.Kaczorowski@int.pan.wroc.pl (D. Kaczorowski).

0925-8388/$ – see front matter © 2012 Elsevier B.V. All rights reserved.
doi:10.1016/j.jallcom.2012.02.100

Table 1
Crystallographic data and experimental conditions for the structure refinements of Ce_3Rh_5Si.

	Ce_3Rh_5Si
Composition, EPMA (at.%)	$Ce_{33.3}Rh_{56.0}Si_{10.7}$
Composition from refinement (at.%)	$Ce_{33.3}Rh_{55.8}Si_{10.9}$
Formula from refinement	$Ce_3Rh_{5.02}Si_{0.98}$
Space group	*Pnma* (No 62)
Pearson symbol	*oP36*
Prototype	Ce_3Rh_5Si
Lattice parameters (nm)	$a = 1.52632(2)$ $b = 0.55092(1)$ $c = 0.75302(1)$
Reflection measured	331
2θ range (°)	$10 \leq 2\theta \leq 90$
Number of variables	21
$R_F = \Sigma\lvert F_o - F_c\rvert / \Sigma F_o$	0.055
$R_I = \Sigma\lvert I_o - I_c\rvert / \Sigma I_o$	0.065
$R_{wP} = [\Sigma w_i \lvert y_{oi} - y_{ci}\rvert^2 / \Sigma w_i \lvert y_{oi}\rvert^2]^{1/2}$	0.055
$R_P = \Sigma\lvert y_{oi} - y_{ci}\rvert / \Sigma\lvert y_{0i}\rvert$	0.043
$R_e = [(N - P + C)/\Sigma w_i y^2_{oi}]^{1/2}$	0.028
$\chi^2 = (R_{wP}/R_e)^2$	3.9

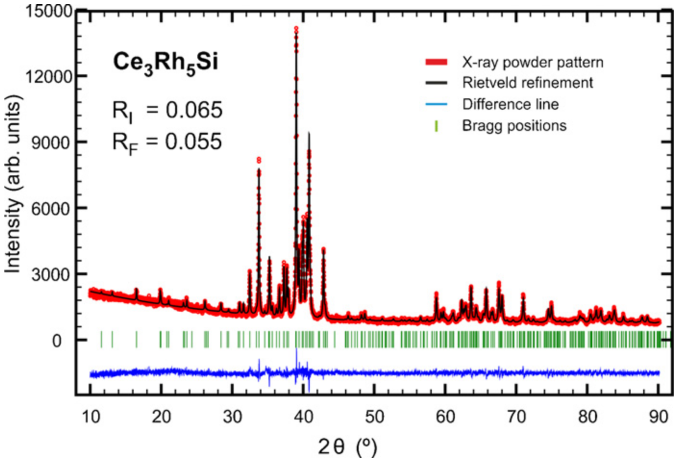

Fig. 1. Powder X-ray diffraction pattern of Ce_3Rh_5Si and its Rietveld refinement.

isotropic displacement parameters that the much more mobile Ce atoms placed inside the voids (see Table 2).

The Ce_3Rh_5Si compound can be considered as a disordered cubic Laves phase. Generally, the phase equilibria in the Ce–Rh–Si system exhibit fairly significant mutual solubility between cerium silicides and cerium–rhodium compounds, and show extended homogeneity ranges of some of the ternaries. These effects seem most clearly observed at 33 at. % of cerium. As pointed out in Ref. [1], up to 6.7 at. % of Si can substitute Rh in the binary compound $CeRh_2$ ($MgCu_2$-type), hence forming the $Ce(Rh_{1-x}Si_x)_2$ phases. With further substitution along that line one obtains the ternary compounds $Ce_3Rh_{5-x}Si_{1+x}$ (Ce_3Rh_5Si-type) and then $Ce_2Rh_{3+x}Si_{1-x}$ (Y_2Rh_3Ge-type), each with its specific homogeneity region. The three series are schematically presented in Fig. 3. Clearly, the substitution of more than 8.5 at. % of Si for the Rh atoms in the parent compound $CeRh_2$ brings about significant distortion of the atomic layers, which leads to lowering of the symmetry of the crystal lattice from cubic to rhombohedral. Further increasing of the Si content results in the formation of regular three dimensional framework of the $[Rh_3Si]$ tetrahedrons, and the crystal structure becomes hexagonal.

3.2. Physical properties

The results of magnetic measurements of the Ce_3Rh_5Si sample are summarized in Fig. 4. Over an extended temperature range down to about 25 K, the magnetic susceptibility is nearly constant and its magnitude is of the order of 10^{-3} emu/(mol Ce). At lower temperatures it rapidly increases. The observed behavior of $\chi_m(T)$ cannot by described by the Curie-Weiss law, but the experimental data may be well approximated in the entire temperature range studied (note the solid line in Fig. 4) by its modified version $\chi_m(T) = \chi_0 + C/(T - \theta_p)$. The parameters derived by least-squares fitting are $\chi_0 = 8.24 \times 10^{-4}$ emu/(mol Ce), $C = 8.67 \times 10^{-3}$ (emu K)/(mol Ce) and $\theta_p = 2.5$ K. The small value of the parameter C corresponds to the effective magnetic moment of 0.26 μ_B per Ce ion. Such a reduced moment cannot be considered as an intrinsic property of Ce_3Rh_5Si but should rather be attributed to small amount of magnetic impurities in the studied sample. Assuming that the latter contribution is mainly due to Ce^{3+} ions located on sample surface and grain boundaries ($\mu_{eff}^{Ce3+} = 2.54\ \mu_B$) one may estimate their concentration to be about 2% per formula unit.

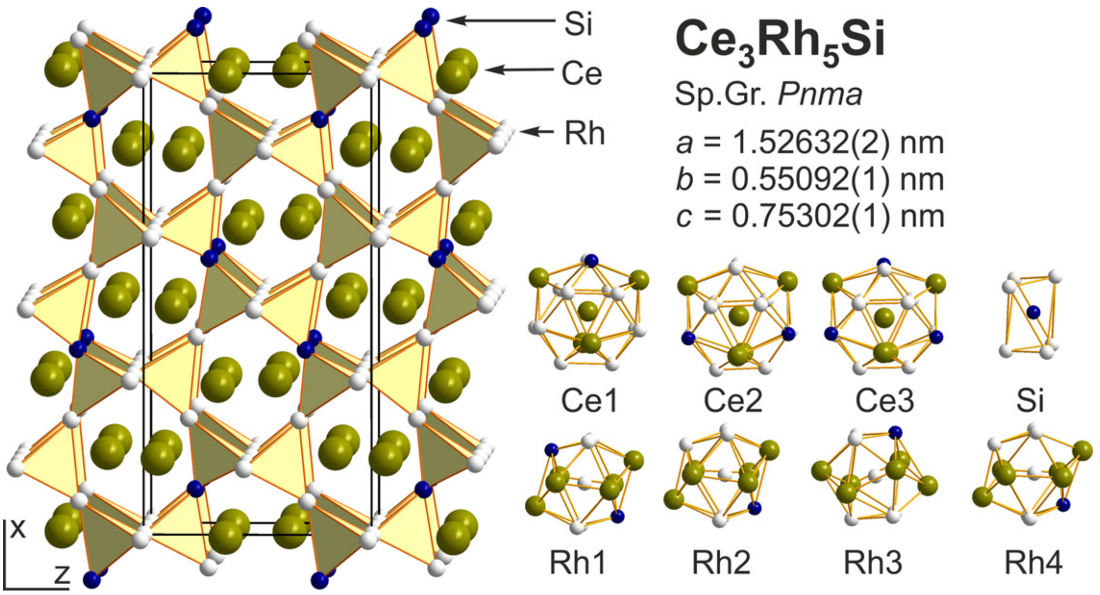

Fig. 2. Crystal structure of Ce_3Rh_5Si and the coordination polyhedra for each type of atom.

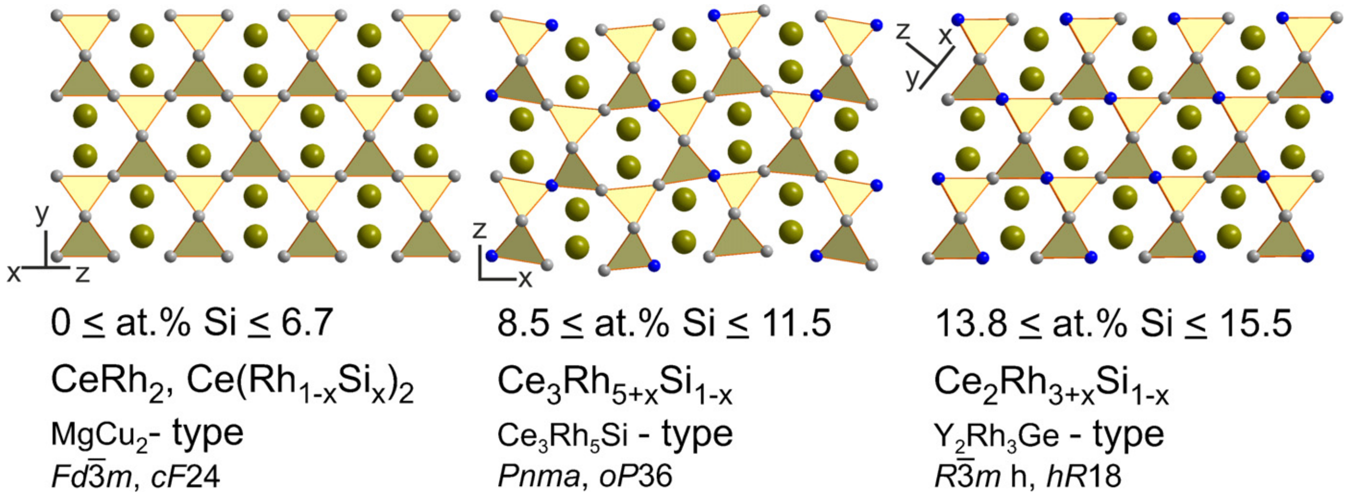

Fig. 3. Comparison of the crystal structures of $CeRh_2$, $Ce_3Rh_{5+x}Si_{1-x}$ and $Ce_2Rh_{3+x}Si_{1-x}$.

Table 2
Atomic coordinates and isotropic thermal displacement parameters (in 10^{-2} nm^2) for Ce_3Rh_5Si. Structure data were standardized with the program STRUCTURE TIDY [5].

Atom	Wycoff position	Occ.	*x*	*y*	*z*	B_{iso}
Ce1	4c	1.0(−)	0.3297(5)	1/4	0.3334(5)	0.70(1)
Ce2	4c	1.0(−)	0.1713(4)	1/4	0.0706(4)	0.73(1)
Ce3	4c	1.0(−)	0.0003(4)	1/4	0.3677(6)	0.63(1)
Rh1	4a	1.0(−)	0	0	0	0.72(1)
Rh2	8d	1.0(−)	0.1549(2)	0.0051(6)	0.4552(4)	0.19(1)
Rh3	4c	1.0(−)	0.0779(5)	1/4	0.7239(7)	0.19(1)
Rh4	4c	1.0(−)	0.2541(5)	1/4	0.6899(8)	0.35(1)
M	4c	0.98(1) Si + 0.02 Rh	0.407(1)	1/4	0.721(2)	0.5(1)

Obviously, such a small amount of secondary phases could not be discriminated in the standard XRD examination.

While the Curie-Weiss-like upturn in $\chi_m(T)$ is associated with the impurity contamination, the temperature independent term χ_0 likely represents the intrinsic Pauli paramagnetism of Ce_3Rh_5Si. Remarkably, its magnitude is very similar to χ_0 reported for some other Ce–Rh–Si ternaries, like $CeRh_{1.82}Si_{0.18}$ and $Ce_2Rh_{3.1}Si_{0.9}$ [6] with the crystal structures closely related to that of Ce_3Rh_5Si (see the discussion above). Apparently, in all these materials the cerium ions are nominally tetravalent and hence possess a nonmagnetic $4f^0$ configuration of their electronic ground state.

In line with the above-outlined interpretation of the magnetic susceptibility data of Ce_3Rh_5Si, the magnetization measured at $T = 1.71$ K as a function of magnetic field (see the inset to Fig. 4) shows a shape characteristic of weakly paramagnetic systems, and its value reached at $\mu_0 H = 5$ T is only 0.44 emu/g, which corresponds to the very small magnetic moment of 0.06 μ_B per formula unit. Clearly, for the most part the latter value should be attributed to the anticipated spurious magnetic phase(s).

Fig. 5 presents the temperature variation of the electrical resistivity of Ce_3Rh_5Si. The compound exhibits a behavior characteristic of nonmagnetic metals. The rather large residual resistivity

Table 3
Interatomic distances (d in nm) and coordination numbers (CN) of the atoms in the crystal structure of Ce_3Rh_5Si ($|\Delta| < 0.0001$ nm).

Atom 1	Atom 2	*d*	Atom 1	Atom 2	*d*	Atom 1	Atom 2	*d*	Atom 1	Atom 2	*d*
Ce1	-1Rh4	0.2922	Ce2	-1Rh3	0.2972	Ce3	-2Rh2	0.2798	Rh1	-2 M	0.2572
CN = 16	-1Ce3	0.3012	CN = 16	-2Rh1	0.3000	CN = 16	-1Rh3	0.2936	CN = 12	-2Rh1	0.2754
	-2Rh2	0.3122		-2Rh4	0.3114		-1Ce1	0.3012		-2Rh3	0.2760
	-1Ce2	0.3123		-1Ce1	0.3123		-2Rh2	0.3060		-2Ce2	0.3000
	-1 M	0.3142		-2Rh2	0.3128		-2Rh3	0.3078		-2Ce3	0.3090
	-2Rh2	0.3188		-1Rh4	0.3130		-2Rh1	0.3090		-2Ce1	0.3201
	-2Rh1	0.3201		-2Rh2	0.3201		-2 M	0.3288			
	-2Rh3	0.3204		-2 M	0.3207		-2Ce3	0.3402	Rh2	-1 M	0.2453
	-2Rh4	0.3221		-2Ce1	0.3282		-1 M	0.3416	CN = 12	-1Rh4	0.2695
	-2Ce2	0.3282		-1Ce3	0.3436		-1Ce2	0.3436		-1Rh2	0.2698
										-1Rh3	0.2706
Rh3	-1 M	0.2632	Rh4	-1 M	0.2351	M	-1Rh4	0.2351		-1Ce3	0.2798
CN = 12	-1Rh4	0.2704	CN = 12	-2Rh2	0.2695	CN = 12	-2Rh2	0.2453		-1Rh4	0.2804
	-2Rh2	0.2706		-1Rh3	0.2704		-2Rh1	0.2572		-1Rh2	0.2810
	-2Rh1	0.2760		-2Rh2	0.2804		-1Rh3	0.2632		-1Ce3	0.3060
	-1Ce3	0.2936		-1Ce1	0.2922		-1Ce1	0.3142		-1Ce1	0.3122
	-1Ce2	0.2972		-2Ce2	0.3114		-2Ce2	0.3207		-1Ce2	0.3128
	-2Ce3	0.3078		-1Ce2	0.3130		-2Ce3	0.3288		-1Ce1	0.3188
	-2Ce1	0.3204		-2Ce1	0.3221		-1Ce3	0.3416		-1Ce2	0.3201

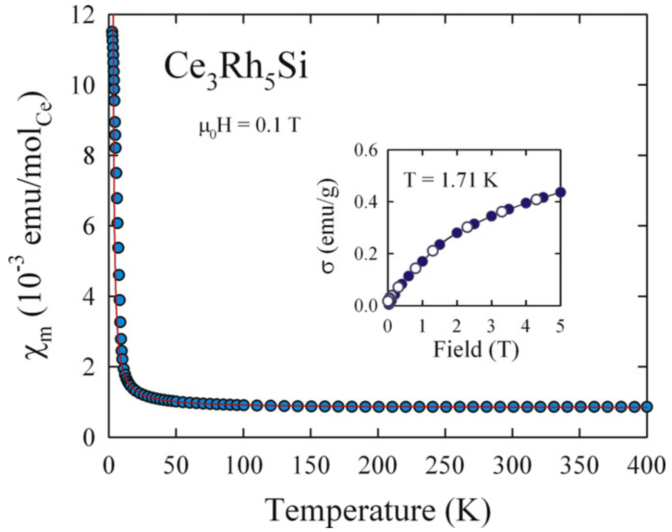

Fig. 4. Temperature dependence of the molar magnetic susceptibility of Ce$_3$Rh$_5$Si. The solid line represents the fit discussed in the text. Inset: field variation of the magnetization measured at 1.71 K with increasing (full circles) and decreasing (open circles) magnetic field strength.

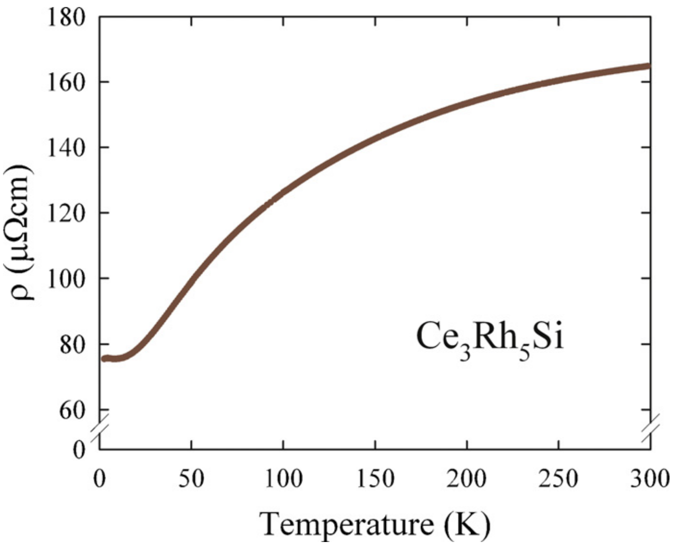

Fig. 5. Temperature dependence of the electrical resistivity of Ce$_3$Rh$_5$Si.

measured at the lowest temperatures ($\rho_0 = 75\,\mu\Omega\,$cm), signalling substantial scattering conduction electrons on static defects in the crystal lattice, may principally result from the structural disorder in the unit cell of Ce$_3$Rh$_5$Si, in which one of the crystallographic sites is occupied by a mixture of Si and Rh atoms (cf. Table 2). Another contribution to ρ_0 may originate from microcracks present in the fairly brittle specimen measured. At higher temperatures, the $\rho(T)$ curve of Ce$_3$Rh$_5$Si is strongly curvilinear. This feature likely manifests significant interband charge scattering of the Mott type, which was evidenced before in the resistivity data of several other Ce–Rh–Si ternaries [6], among them for the closely related compound CeRh$_{1.82}$Si$_{0.18}$.

4. Conclusions

The novel ternary compound Ce$_3$Rh$_5$Si crystallizes with the orthorhombic crystal structure (space group *Pnma*) of its own type. The cerium atoms, located in the unit cell at three crystallographically inequivalent sites, possess nonmagnetic $4f^0$ configuration that brings about weak Pauli paramagnetic behavior. The compound exhibits metallic character of the electrical conductivity with probable significant contribution due to the Mott-type scattering.

Acknowledgment

This work was financially supported by the Russian Foundation for Basic Research (RFBR) under grants No. 11-03-00957 and No. 11-03-01191.

References

[1] A. Lipatov, et al., J. Solid State Chem. 183 (2010) 829.
[2] STOE WINXPOW (Version 1.06), Stoe & Cie GmbH, Darmstadt, Germany, 1999.
[3] J. Rodriguez-Carvajal, FULLPROF: A Program for Rietveld Refinement and Pattern Matching Analysis, in Abstracts of the Satellite Meeting on Powder Diffraction of the XV Congress of the IUCr, Toulouse, France, 1990, p. 127.
[4] L. Palatinus, G. Chapuis, J. Appl. Cryst. 40 (2007) 786.
[5] E. Parthe, et al., TYPIX Standardized Data and Crystal Chemical Characterization of Inorganic Structure Types, Springer-Verlag, Berlin, Heidelberg, 1994.
[6] D. Kaczorowski, et al., J. Alloys Compd. 509 (2011) 6518.